

What Image Properties Regulate Eye Growth?

Robert F. Hess,^{1,*} Katrina L. Schmid,²
Serge O. Dumoulin,³ David J. Field,⁴
and Darren R. Brinkworth²

¹McGill Vision Research
Department of Ophthalmology
McGill University
Montreal, Quebec H3A 1A1
Canada

²School of Optometry
Institute of Health and Biomedical Innovation
Queensland University of Technology
Brisbane, Queensland Q4059
Australia

³Department of Psychology
Stanford University
Stanford, California 94305

⁴Department of Psychology
Cornell University
Ithaca, New York 14853

Summary

The growth of the eye, unlike other parts of the body, is not ballistic. It is guided by visual feedback with the eventual aim being optimal focus of the retinal image or emmetropization [1]. It has been shown in animal models that interference with the quality of the retinal image leads to a disruption to the normal growth pattern, resulting in the development of refractive errors and defocused retinal images [1, 2]. While it is clear that retinal images rich in pattern information are needed to control eye growth, it is unclear what particular aspect of image structure is relevant. Retinal images comprise a range of spatial frequencies at different absolute and relative contrasts and in different degrees of spatial alignment. Here we show, by using synthetic images, that it is not the local edge structure produced by relative spatial frequency alignments within an image but rather the spatial frequency composition per se that is used to regulate the growth of the eye. Furthermore, it is the absolute energy at high spatial frequencies regardless of the spectral slope that is most effective. Neither result would be expected from currently accepted ideas of how human observers judge the degree of image “blur” in a scene where both phase alignments [3] and the relative energy distribution across spatial frequency [4] (i.e., spectral slope) are important.

Results and Discussion

A number of studies have been directed toward understanding what aspects of an image might affect eye growth regulation (e.g., contrast, spatial content, color,

and luminance [5–10]). Many studies have introduced controlled amounts of optical defocus and have elegantly demonstrated that the eye grows to minimize image blur [11–15]. Recent research has provided fresh insights into how we detect image blur by highlighting the importance of the relative contrast at different spatial frequencies rather than just the absolute contrast at high spatial frequencies. For example, natural images have common shaped Fourier amplitude spectra, falling inversely with spatial frequency [16], and it has been shown that our perception of image blur depends on deviations from this common form [3, 4]; *images with sharper spectral fall-offs appear more blurred regardless of their absolute high spatial frequency content*. This leads to the question of whether eye growth depends on the absolute or relative energy at high image spatial frequencies. A related issue involves the importance of edge structure in images. An edge represents a particular alignment of frequencies as well as a particular ratio of energies, and we describe two studies: the first explores whether the alignment of energy (i.e., phase alignment) at different spatial frequencies plays an important role in regulating eye growth, and the second determines whether it is the relative or absolute energy at different frequencies that is important.

Our two experiments explore how these two independent components of natural images contribute to the regulation of eye growth. The first issue relates to the importance of the phase spectrum and in particular phase alignments that commonly occur in natural images. These have been implicated in our detection of image blur [17] and our identification of objects [18, 19], and they could potentially play a key role in the regulation of eye growth. The second issue relates to the importance of the shape of the amplitude spectra of natural images (i.e., $1/f$ fall-off) and the possible use of deviations from this common shape to drive both our perception of image blur and regulation of eye growth. To resolve these issues, we reared chickens, a well-established animal model in eye-growth research [20], under controlled conditions where the local and global properties of synthetic images that they viewed during early life could be manipulated. On day 8 after birth, a cone-shaped imaging system, giving a 60° view of an optically focused target (+30 D lens viewing a target at 3.3 cm and having minimal aberrations [21]), was applied monocularly to the chicks’ right eyes [10]. The details of this cone system, how spectacle lens magnification was taken into account in the target parameters and how the targets were produced, are given elsewhere [21]. Since the eyes of these infant animals are actively growing, the prediction is that only a target providing sufficient information will allow the eyes to grow correctly and maintain the eyes at a refraction around emmetropia. Targets with no spatial information (i.e., blank targets) produce uncontrolled eye growth and high levels of myopia in young chicks; up to 0.5 mm of axial elongation (~10% increase in vitreous chamber

*Correspondence: robert.hess@mcgill.ca

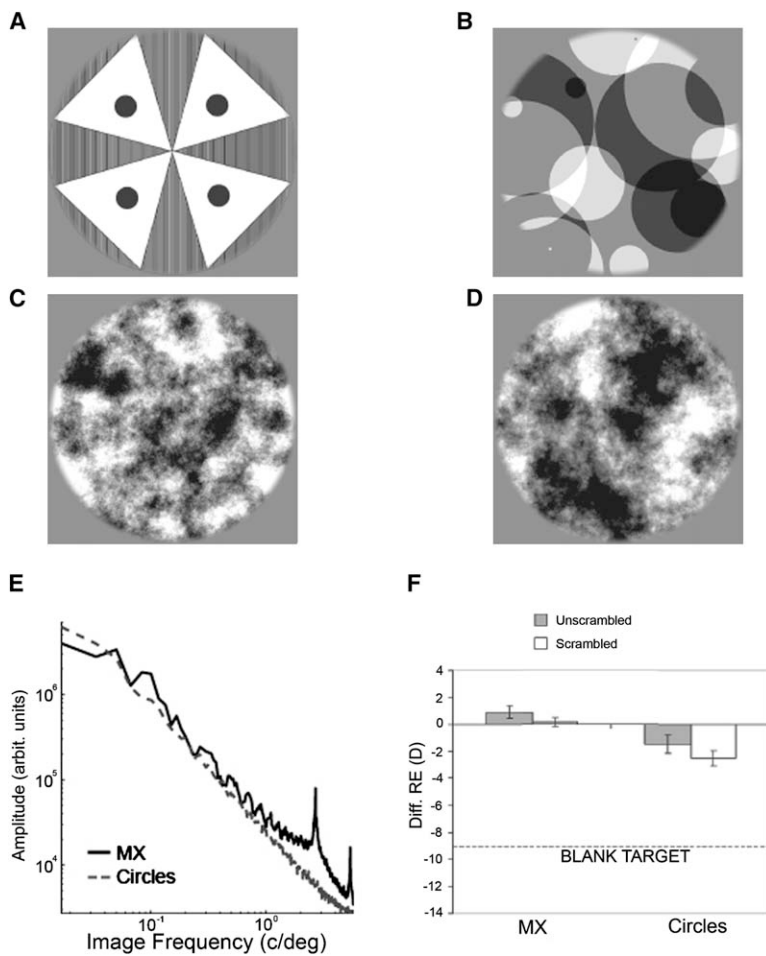


Figure 1. Effect of Image Features

In (A) and (B), two targets are shown that are rich in high-contrast spatial features and both have a $1/f$ spatial frequency spectrum (see [E]). In (C) and (D), versions of (A) and (B) are shown in which the respective phase spectra have been randomized. These scrambled versions contain the same amplitude spectra as (A) and (B) but none of the local phase alignments that represent local spatial features. In (F), the results (\pm SE; $n = 8$) are shown for the effectiveness of each of the above four targets (A–D) for producing emmetropization in the growth pattern for the chick eye (0 dioptres represents perfect compensation). The dashed line represents the result if a blank target is used to restrict visual feedback. Although the Maltese cross pattern is more effective, the scrambled versions are just as effective as their unscrambled counterparts, suggesting that the phase spectrum is not used in regulating eye growth.

depth) and 10 D of myopia with 4 days of treatment [21]. After 4.5 days of controlled rearing, measurements of refractive error were made by streak retinoscopy and A-scan ultrasonography. The targets were static (i.e., nonmoving), and the chicks could move their eyes under the lens. We used information on the most recent behavioral measure of visual acuity in the chick (~ 7 to 8 cyc/deg) in designing the high spatial frequency cut-off of the targets [22]. Due to the very short target distance and high-powered positive lens used, small errors in lens and target position can alter the amount of defocus on the target (e.g., 1 D for 1 mm change). In addition, the refractive error of chicks at the time treatment commenced (usually 2–3 D of hyperopia [21]) would further alter the amount of defocus experienced. However, these errors would affect all targets equally. Based on our past experience with this system, isometropia to 1.5 D of relative hyperopia should be measured for a target with properties that meet the criteria for accurate emmetropization [21]. Each chick was exposed to only one target for the treatment period (total $n = 167$; 6 to 12 chicks per treatment group as indicated in figure captions). Data presented are mean (\pm SE) interocular differences (treated minus untreated). Statistical analysis was conducted with factorial ANOVAs and Tukey post-hoc tests in the Statistical Package for the Social Sciences (SPSS). Experiments were conducted in accordance with the “Australian code of practice for the

care and use of animals for scientific purposes” of the NHMRC.

Figures 1A–1D show the four images used to answer the first question pertaining to the importance of local image features (and by implication, the phase spectra) in the regulation of eye growth. The top images (Figures 1A and 1B) are rich in features and have highly structured phase spectra. The images below (Figures 1C and 1D) are phase-scrambled versions of the two above. All images (Figures 1A–1D) have similar amplitude spectra that fall off as $1/\text{image spatial frequency}$ (see Figure 1E). The results in Figure 1F show the eye growth effects, quantified in dioptres of induced defocus (0 representing perfect compensation), produced by restricting the vision of developing chicks to one or other of these patterns. The dashed line is the result obtained with an occluder (i.e., blank target) and represents the expected result if there is no visual feedback to regulate eye growth. Within the accuracy of our measurements, we could not find any difference in the emmetropia maintaining ability of images whose phase spectra were scrambled (filled and unfilled blocks in Figure 1F; refractive error interocular difference: MX unscrambled versus scrambled, $p = 0.99$; circles unscrambled versus scrambled, $p = 0.94$). Although the unscrambled MX target was slightly superior at preventing axial elongation than its scrambled version (axial length interocular difference: MX unscrambled -0.11 ± 0.14 mm versus

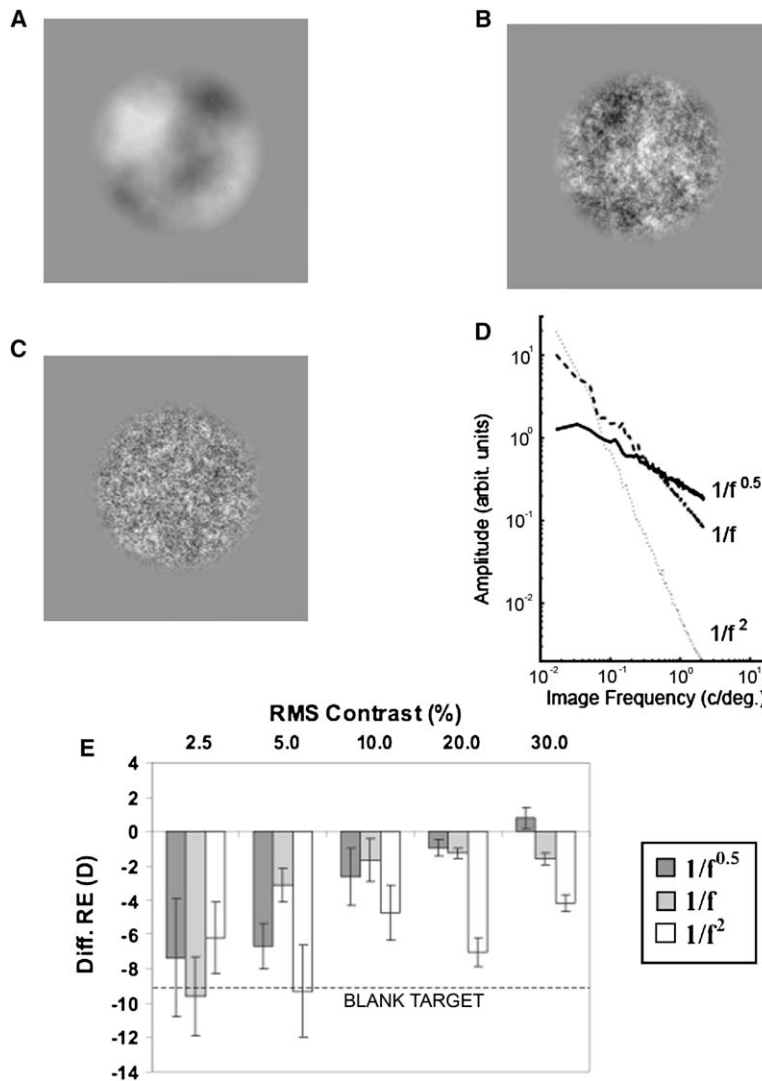


Figure 2. Effect of Spectral Fall-Off

In (A)–(C), three fractal noise patterns of equal RMS contrast energy are shown in which the slope of the spectral fall-off varies from $1/f^{0.5}$ to $1/f^2$. Their spectra are shown in (D). In (E), the results (\pm SE) of the effectiveness of these patterns for producing emmetropic growth patterns (0 dioptres represents perfect compensation) for the developing chick eye. Results are compared for each of the three spectral fall-offs as a function of the overall matched contrast energy level. The dashed line represent the result if blank target is used to restrict visual feedback. As the overall energy level increases, the eye growth patterns become more emmetropic and the noise pattern with the higher spatial frequency content is more effective. Sample size ($f = 0.5, 1, 2$) = 2.5% 6,8,8; 5% 7,8,8; 10% 12,12,12; 20% 9,9,9; 30% 9,9,9.

scrambled 0.09 ± 0.10 mm, $p < 0.05$), the unscrambled circle target wasn't (0.18 ± 0.12 mm versus scrambled 0.27 ± 0.08 mm, $p = 0.52$). Also, both scrambled targets significantly inhibited the myopia and axial elongation seen with a blank target (blank: refractive error interocular difference -9.11 ± 4.68 D, axial length interocular difference 0.40 ± 0.22 mm, $p < 0.05$ for all comparisons with the scrambled targets) A small, though statistically significant ($p < 0.05$), difference in axial inhibition ability was found between the Maltese cross and circles stimulus that may have been in part due to an additional high (~ 2 cpd) spatial frequency spike in the Maltese cross produced by the background stripes (Figure 1A and spike in solid curve in Figure 1E). These results suggests that phase alignments within an image that determine the perceived local spatial features in the images shown in Figures 1A and 1B are not crucial in the visual feedback regulation of eye growth.

Since the amplitude spectrum provides sufficient information for the emmetropization process, we wondered if the fractal (i.e., an amplitude spectrum with a $1/\text{image}$ spatial frequency fall-off) nature of natural images was optimal for the regulation of eye growth as

it is for blur perception [3, 4]. To answer this, we reared chicks viewing the 2D noise images shown in Figures 2A–2C in which both the spectral fall-off ($1/f^{0.5}$ – $1/f^2$; see spectra in Figure 2D) and the overall contrast energy (i.e., the root-mean-squared pixel values) were independently varied. This allowed us to assess whether it is the absolute or relative energy in different spatial frequency bands that regulates eye growth. We found that both the contrast energy of the target and the spectral fall-off were important determinants of the ability of the target to guide emmetropization (contrast energy: refractive error difference $F_{4,135} = 7.704$, $p < 0.001$, axial length difference $F_{4,135} = 7.104$, $p < 0.001$; spectral fall-off: refractive error difference $F_{2,135} = 5.841$, $p < 0.005$, axial length difference $F_{2,135} = 12.699$, $p < 0.001$). However, from the results shown at a number of fixed contrast energies, it can be seen that there is no good evidence for $1/f$ being optimal for growth regulation. At the higher energy levels allowed by the experimental method, the least effective stimulus was the $1/f^2$, whereas the most effective was $1/f^{0.5}$ (refractive error interocular difference: $1/f^{0.5}$ 0.81 ± 1.87 D versus $1/f^2$ -4.15 ± 1.47 D, $p < 0.005$; axial length interocular difference: $1/f^{0.5}$ 0.08 ± 0.13 mm

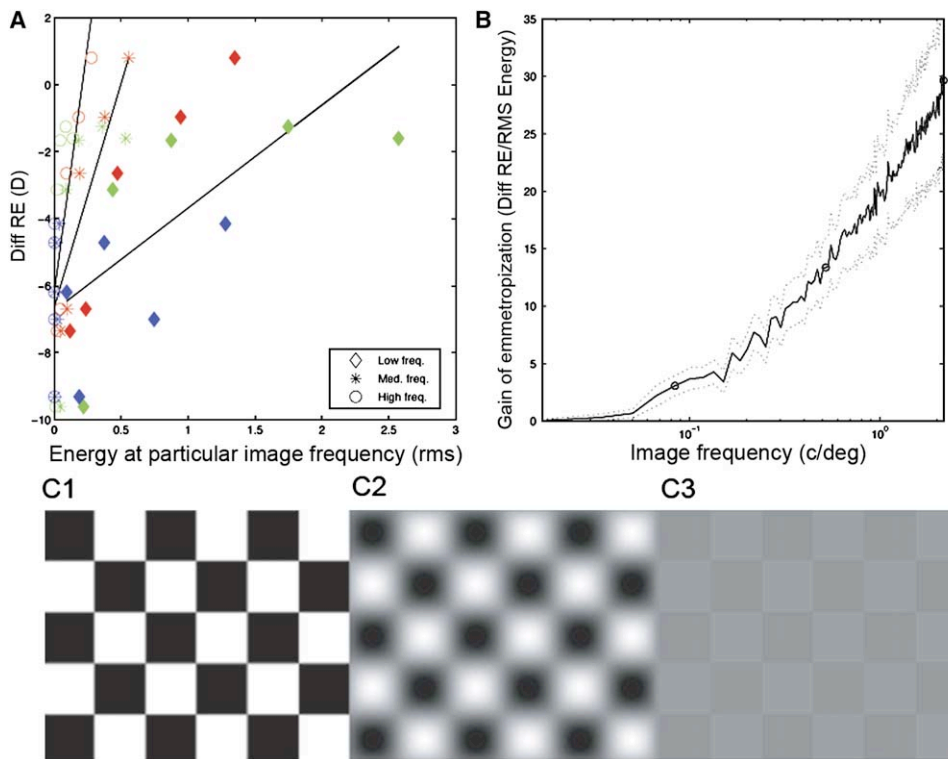


Figure 3. Effect of Image Frequency

In (A), the data for the noise patterns with the three spectral slopes in Figures 2A–2C are replotted in different colors (green, $1/f$; blue, $1/f^2$; red, $1/f^{0.5}$) as a function of energy for three different spatial frequencies (low, medium, high) and fitted by straight lines. In (B), the slopes of these lines (\pm SD), which represent the rate of emmetropization, are plotted against image frequency. Higher image frequencies are more effective in producing emmetropization. In (C), the original checkerboard image in C1 has been altered in two different ways. Either its spectral slope has been steepened to produce a blurred replica (C2) or its contrast has been scaled to produce the low contrast replica (C3). Both (C2) and (C3) have identical energy at high spatial frequencies and will therefore, on the basis of the current results, be equally effective in regulating eye growth, though only C2 is *perceived* to be “blurred.”

versus $1/f^2$ 0.37 ± 0.12 mm, $p < 0.01$). Thus, it appears that images with higher absolute energy at mid and high spatial frequencies are better. This is best seen by replotting these data (the three different spectral fall-offs at the three energy levels) as a function of the absolute energy at different spatial frequencies (Figure 3). In Figure 3A, as an example, we plot emmetropization versus image energy at each of three image frequencies: a low, medium, and high image frequency (0.084, 0.5207, 2.1667 c/deg). In Figure 3B, we replot all the data (all spatial frequencies) of Figure 2E as a function of the rate at which emmetropization occurs (i.e., the slope in Figure 3A). The gain of the emmetropization process is seen to directly depend on the absolute energy contained at higher image frequencies. Mid spatial frequencies that have been shown to be effective in previous studies [7, 21, 23] are not as effective as high spatial frequencies. What makes this finding unexpected is that our perception of what is blurred is known to be governed not by the absolute energy at high spatial frequencies within an image but rather by how the energy is distributed across spatial frequency [3, 4] (i.e., the relative energy or spectral slope). Figure 3C illustrates this: the stimulus with the altered spectral slope (C2) appears blurred, whereas the image with the scaled contrast (C3) does not, yet both images, according to our data in Figure 3B, are equally effective in regulating eye growth

because they both have the same absolute energy at high spatial frequencies.

Since the eye receives only limited feedback [24] (e.g., there are only limited contralateral effects [25, 26]) from higher processing areas of the visual pathway, we know that regulation of eye growth predominately originates in the eye [27, 28], not the cortex. Unlike the results found for the perception of blur, the results of this study imply that a relatively simple function of retinal activity may be sufficient to model the magnitude (but not the sign) of emmetropization in the chick. Since the absolute energy at the higher spatial frequencies determines the degree of emmetropization (i.e., the extent to which the growth of the eye compensates for the refractive error), we conclude that the total activity in possibly a subset of retinal cells (e.g., amacrine cells) responding in the higher spatial frequency range may be sufficient to drive the emmetropization process. Although the slope of the spectrum and the sparse structure in images plays a role in the *perception* of blur, we find no evidence that these properties play a role in the *growth* of the eye.

Acknowledgments

This work was supported by ARC Research Grant number A10024102 to K.L.S. and CIHR (# MT 108-18) grant to R.F.H. We

are very grateful to Bruce Hansen for his help in manuscript preparation, particularly [Figure 3C](#).

Received: December 14, 2005

Revised: February 13, 2006

Accepted: February 14, 2006

Published: April 3, 2006

References

1. Wallman, J., Turkel, J., and Trachtman, J. (1978). Extreme myopia produced by modest change in early visual experience. *Science* *201*, 1249–1251.
2. Hodos, W., and Kuenzel, W.J. (1984). Retinal image degradation produces ocular enlargement in chicks. *Invest. Ophthalmol. Vis. Sci.* *25*, 652–659.
3. Field, D.J., and Brady, N. (1997). Visual sensitivity, blur and the sources of variability in the amplitude spectra of natural scenes. *Vision Res.* *37*, 3367–3383.
4. Webster, M.A., Georgeson, M.A., and Webster, S.M. (2002). Neural adjustments to image blur. *Nat. Neurosci.* *5*, 839–840.
5. Wildsoet, C.F., Howland, H.C., Falconer, S., and Dick, K. (1993). Chromatic aberration and accommodation: their role in emmetropization in the chick. *Vision Res.* *33*, 1593–1603.
6. Bartmann, M., and Schaeffel, F. (1994). A simple mechanism for emmetropization without cues from accommodation or colour. *Vision Res.* *34*, 873–876.
7. Schmid, K.L., and Wildsoet, C.F. (1997). Contrast and spatial-frequency requirements for emmetropization in chicks. *Vision Res.* *37*, 2011–2021.
8. Schaeffel, F., and Diether, S. (1999). The growing eye: an autofocus system that works on very poor images. *Vision Res.* *39*, 1585–1589.
9. Diether, S., Gekeler, F., and Schaeffel, F. (2001). Changes in contrast sensitivity induced by defocus and their possible relations to emmetropization in the chicken. *Invest. Ophthalmol. Vis. Sci.* *42*, 3072–3079.
10. Wildsoet, C.F., and Schmid, K.L. (2001). Emmetropization in chicks uses optical vergence and relative distance cues to decode defocus. *Vision Res.* *41*, 3197–3204.
11. Schaeffel, F., Glasser, A., and Howland, H.C. (1988). Accommodation, refractive error and eye growth in chickens. *Vision Res.* *28*, 639–657.
12. Irving, E.L., Callender, M.G., and Sivak, J.G. (1991). Inducing myopia, hyperopia, and astigmatism in chicks. *Optom. Vis. Sci.* *68*, 364–368.
13. Norton, T.T., and Sieglwart, J.T. (1995). Animal models of emmetropization: matching axial length to the focal plane. *J. Am. Optom. Assoc.* *66*, 405–414.
14. Smith, E.L., 3rd, and Hung, L.F. (1999). The role of optical defocus in regulating refractive development in infant monkeys. *Vision Res.* *39*, 1415–1435.
15. Winawer, J., Zhu, X., Choi, J., and Wallman, J. (2005). Ocular compensation for alternating myopic and hyperopic defocus. *Vision Res.* *45*, 1667–1677.
16. Field, D.J. (1987). Relations between the statistics of natural images and the response properties of cortical cells. *J. Opt. Soc. Am. A* *4*, 2379–2394.
17. Hess, R.F., Pointer, J.S., and Watt, R.J. (1989). How are spatial filters used in fovea and parafovea? *J. Opt. Soc. Am. A* *6*, 329–339.
18. Oppenheim, A.V., and Lim, J.S. (1981). The importance of phase in signals. *Proc. IEEE* *69*, 529–541.
19. Piotrowski, L.N., and Campbell, F.W. (1982). A demonstration of the visual importance and flexibility of spatial frequency amplitude and phase. *Perception* *11*, 337–346.
20. Wallman, J. (1993). Retinal control of eye growth and refraction. In *Progress in Retinal Research*, Volume 12, N. Osbourne and G. Chader, eds. (Oxford: Pergamon Press), pp. 133–153.
21. Schmid, K.L., Brinkworth, D.R., Wallace, K.M., and Hess, R.F. (2006). The effect of manipulations to target contrast on emmetropization in chick. *Vision Res.* *46*, 1099–1107.
22. Schmid, K.L., and Wildsoet, C.F. (1998). Assessment of visual acuity and contrast sensitivity in the chick using an optokinetic nystagmus paradigm. *Vision Res.* *38*, 2629–2634.
23. Diether, S., and Wildsoet, C.F. (2005). Stimulus requirements for the decoding of myopic and hyperopic defocus under single and competing defocus conditions in the chicken. *Invest. Ophthalmol. Vis. Sci.* *46*, 2242–2252.
24. Bitzer, M., and Schaeffel, F. (2006). ZENK expression of retinal glucagon amacrine cells in chicks: the effect of defocus presented in vivo, in vitro and under anesthesia. *Vision Res.* *46*, 848–859.
25. Wildsoet, C.F., and Wallman, J. (1995). Choroidal and scleral mechanisms of compensation to spectacle lenses in chicks. *Vision Res.* *35*, 1227–1245.
26. Gentle, A., and McBrien, N.A. (2003). Is the contralateral control eye abnormal in myopia research? *Clin. Exp. Optom.* *87*, 51–52.
27. Troilo, D., Gottlieb, M.D., and Wallman, J. (1987). Visual deprivation causes myopia in chicks with optic nerve section. *Curr. Eye Res.* *6*, 993–999.
28. Wildsoet, C.F., and Pettigrew, J.D. (1988). Kainic acid-induced eye enlargement in chickens: differential effects on anterior and posterior segments. *Invest. Ophthalmol. Vis. Sci.* *29*, 311–319.